ADVANCES IN ATMOSPHERIC SCIENCES, VOL. 37, DECEMBER 2020, 1297–1309

• **Original Paper** •

Comparison of Ozone and $PM_{2.5}$ Concentrations over Urban, Suburban, and Background Sites in China

Lan GAO[1,2], Xu YUE[*3], Xiaoyan MENG[4], Li DU[4], Yadong LEI[1,2], Chenguang TIAN[1,2], and Liang QIU[1,2,5]

[1]*Climate Change Research Center*, *Institute of Atmospheric Physics*, *Chinese Academy of Sciences*, *Beijing* 100029, *China*

[2]*University of Chinese Academy of Sciences*, *Beijing* 100049, *China*

[3]*Jiangsu Key Laboratory of Atmospheric Environment Monitoring and Pollution Control*, *Collaborative Innovation Center of Atmospheric Environment and Equipment Technology*, *School of Environment Science and Engineering*, *Nanjing University of Information Science & Technology*, *Nanjing* 210044, *China*

[4]*China National Environmental Monitoring Center*, *Beijing* 100012, *China*

[5]*School of Atmospheric Sciences*, *Chengdu University of Information and Technology*, *Chengdu* 610225, *China*

(Received 2 March 2020; revised 5 August 2020; accepted 1 September 2020)

ABSTRACT

Surface ozone (O_3) and fine particulate matter ($PM_{2.5}$) are dominant air pollutants in China. Concentrations of these pollutants can show significant differences between urban and nonurban areas. However, such contrast has never been explored on the country level. This study investigates the spatiotemporal characteristics of urban-to-suburban and urban-to-background difference for O_3 ($\Delta[O_3]$) and $PM_{2.5}$ ($\Delta[PM_{2.5}]$) concentrations in China using monitoring data from 1171 urban, 110 suburban, and 15 background sites built by the China National Environmental Monitoring Center (CNEMC). On the annual mean basis, the urban-to-suburban $\Delta[O_3]$ is −3.7 ppbv in Beijing–Tianjin–Hebei, 1.0 ppbv in the Yangtze River Delta, −3.5 ppbv in the Pearl River Delta, and −3.8 ppbv in the Sichuan Basin. On the contrary, the urban-to-suburban $\Delta[PM_{2.5}]$ is 15.8, −0.3, 3.5 and 2.4 μg m^{-3} in those areas, respectively. The urban-to-suburban contrast is more significant in winter for both $\Delta[O_3]$ and $\Delta[PM_{2.5}]$. In eastern China, urban-to-background differences are also moderate during summer, with −5.1 to 6.8 ppbv for $\Delta[O_3]$ and −0.1 to 22.5 μg m^{-3} for $\Delta[PM_{2.5}]$. However, such contrasts are much larger in winter, with −22.2 to 5.5 ppbv for $\Delta[O_3]$ and 3.1 to 82.3 μg m^{-3} for $\Delta[PM_{2.5}]$. Since the urban region accounts for only 2% of the whole country's area, the urban-dominant air quality data from the CNEMC network may overestimate winter $[PM_{2.5}]$ but underestimate winter $[O_3]$ over the vast domain of China. The study suggests that the CNEMC monitoring data should be used with caution for evaluating chemical models and assessing ecosystem health, which require more data outside urban areas.

Key words: ozone, $PM_{2.5}$, urban, suburban, background

Citation: Gao, L., X. Yue, X. Y. Meng, L. Du, Y. D. Lei, C. G. Tian, and L. Qiu, 2020: Comparison of ozone and $PM_{2.5}$ concentrations over urban, suburban, and background sites in China. *Adv. Atmos. Sci.*, **37**(12), 1297–1309, https://doi.org/10.1007/s00376-020-0054-2.

Article Highlights:

- The urban-to-suburban and urban-to-background annual mean differences of O_3 are −3.8 to 1.0 ppbv and −10.4 to 9.9 ppbv, respectively.
- The urban-to-suburban and urban-to-background annual mean differences of $PM_{2.5}$ are −0.3 to 15.8 μg m^{-3} and 3.0 to 47.3 μg m^{-3}, respectively.
- The urban-to-suburban and urban-to-background pollution exhibits seasonal variations, with more significant differences in winter.
- Both O_3 and $PM_{2.5}$ are higher in urban areas than suburbs during pollution episodes in Beijing–Tianjin–Hebei.

* Corresponding author: Xu YUE
Email: yuexu@nuist.edu.cn

1. Introduction

Surface ozone (O_3) and fine particulate matter ($PM_{2.5}$) are two major pollutants in China (Qu et al., 2018; Shu et al., 2019). O_3 is formed by photochemical reactions between nitrogen oxides (NO_x) and volatile organic compounds (VOCs) (Sillman, 1999). Short-term exposure to high O_3 levels can increase the risk of respiratory and cardiovascular mortality, and long-term exposure even at low levels can affect human health (Turner et al., 2016; Mills et al., 2018). In addition, high O_3 concentrations ($[O_3]$) dampen leaf photosynthesis through stomatal uptake, inhibiting plant growth (Gregg et al., 2003) and decreasing ecosystem productivity (Yue et al., 2017). The exposure in China is greater than other, developed countries such as the U.S., Europe, and Japan (Lu et al., 2018). $PM_{2.5}$ is another major pollutant in China, especially in urban areas, due to high local emissions and regionally transported aerosols (Zhang and Cao, 2015). Haze episodes with high $PM_{2.5}$ concentrations ($[PM_{2.5}]$) can cause adverse health problems (Chow, 2006; Pope III and Dockery, 2013) and reduce net primary productivity of plants by limiting radiation and precipitation (Yue et al., 2017).

Observations have shown large differences in air pollution between urban (cities and megacities) and nonurban (suburban, rural, background, and remote) areas. In urban areas, greater volumes of traffic and residential activities increase anthropogenic emissions, such as carbon dioxide (CO_2) and NO_x (Gregg et al., 2003; Pataki et al., 2006). In addition, the greater density of roads and buildings in urban areas changes the surface albedo and heat capacity, causing stronger heat-island effects than in nonurban areas (George et al., 2007). These differences can have substantial impacts on the contrast of O_3 and $PM_{2.5}$ between urban and nonurban regions. Studies have shown that nonurban $[O_3]$ are usually higher than those in urban areas (Dueñas et al., 2004; Banan et al., 2013; Han et al., 2013; Yang et al., 2014; Tong et al., 2017). However, exceptions are also found in that the summer average $[O_3]$ in urban Beijing is 33.4 ± 0.4 ppbv higher than in clean regions (Ge et al., 2012). Model results show that nonurban O_3 is sensitive to NO_x, while urban O_3 is sensitive to both NO_x and VOCs (Sillman et al., 1993; Xing et al., 2011; Jin and Holloway, 2015; Wang et al., 2017), leading to large uncertainties in the urban-to-nonurban difference of O_3 ($\Delta[O_3]$). The urban-to-nonurban difference of $PM_{2.5}$ ($\Delta[PM_{2.5}]$) is less complicated. With more primary and secondary pollutants produced in cities, the urban $PM_{2.5}$ level is usually higher than that in nonurban areas (Putaud et al., 2004; Barmpadimos et al., 2011; Bravo et al., 2016; Xu et al., 2016; Zheng et al., 2018).

In previous studies, the difference in air pollution between urban and nonurban areas has tended to be explored for a city (Han et al., 2013; Wang et al., 2015; Tong et al., 2017; Huang et al., 2018; Zheng et al., 2018; Zhao et al., 2019), several cities (Xue et al., 2014), or a certain region, such as the North China Plain (Xu et al., 2016), Yangtze River Delta (An et al., 2015), or Pearl River Delta (Zheng et al., 2010). However, the urban-to-suburban difference has not been compared among different regions. Since the year 2013, more and more suburban sites have been built to monitor regional pollution levels in contrast to urban sites. In this study, we investigate the differences of O_3 and $PM_{2.5}$ between urban and suburban areas in China using observations from a ground-based monitoring network during 2015–18. We pay particular attention to the spatial distribution and temporal characteristics of such differences. In addition, we use pollution data from 15 background sites built by the China National Environmental Monitoring Center (CNEMC) to compare O_3 and $PM_{2.5}$ concentrations over urban, suburban, and background sites in China. Details regarding the monitoring network are explained in the next section. Section 3 compares the pollution levels between urban and suburban areas, and attempts to interpret the causes. Section 4 compares the pollutant concentrations of urban and suburban sites with those of background sites. And lastly, section 5 discusses and concludes the study's main findings.

2. Data and methods

2.1. *Site-level data*

We use data from the CNEMC of China, including concentrations of O_3, $PM_{2.5}$, NO_2 and SO_2 from 1614 observation sites (http://www.cnemc.cn/sssj/). The time span of these sites ranges from 1 January 2015 to 31 December 2018. For data quality control, we choose 1281 sites with less than 20% missing data for O_3 and $PM_{2.5}$ during the monitoring period, thus ensuring these sites have relatively complete records during 2015–18. In addition, we use the daily maximum 8-h-average O_3 concentrations ([MDA8]) and $PM_{2.5}$ concentrations of background sites in 2017.

According to the requirements by the Ministry of Ecology and Environment (MEE, http://www.mee.gov.cn/), the national ambient air quality monitoring network includes three types of sites, including evaluation, comparison and background sites. Evaluation sites are obliged to be built in urban areas and distributed equally to cover the whole city. Comparison sites are built more than 20 km away from main pollution sources and urban centers, and background sites are built even farther (> 50 km) away. As is shown in Fig. 1, there are 1171 urban sites (evaluation sites), 110 suburban sites (comparison sites), and 15 background sites. The sites are densely located in the central and eastern parts of China, while those in the west and northeast are sparsely distributed. The locations of urban and suburban sites seem to overlap because they are usually only around 20 km away from each other. Most of the background sites are located in natural scenic areas, almost completely free of anthropogenic emissions.

2.2. *Gridded data*

CO_2 and NO_x emissions are good indicators of anthropogenic activities (Gregg et al., 2003; Pataki et al., 2006). We

use emissions data of CO_2 and NO_x from the Multiresolution Emissions Inventory for China (MEIC, http://meicmodel.org) in 2016, which has a resolution of 0.25° × 0.25°. MEIC is a bottom-up emissions inventory that provides anthropogenic emissions of over 700 sources in China using a technology-based method (Li et al., 2019). We derive site-level emissions from MEIC through their locations, and compare their differences between urban and suburban sites.

2.3. *Four selected regions*

We select four megacity clusters in China—namely, Beijing–Tianjin–Hebei (BTH), Yangtze River Delta (YRD), Pearl River Delta (PRD), and Sichuan Basin (SCB)—as the major domains for analysis. These clusters have also been highlighted by the Chinese government as needing to reduce their air pollution (Li et al., 2019). BTH includes 9 cities with 65 urban sites and 5 suburban sites; YRD includes 26 cities with 110 urban sites and 9 suburban sites; PRD includes 9 cities with 50 urban sites and 2 suburban sites; and SCB includes 21 cities with 75 urban sites and 14 suburban sites (Fig. S1 in the Electronic Supplementary Material, ESM). We use all of the urban and suburban sites to compare and quantify the pollutant concentrations within a region.

3. Results

3.1. *Comparison of urban and suburban emissions*

We compare the probability density function (PDF) of CO_2 and NO_x emissions between the urban and suburban CNEMC sites (Fig. 2). For CO_2, 76% of suburban sites show emissions lower than 10000 t km^{-2} yr^{-1}, and this percentage is higher than that of urban sites (65%). In contrast, 19% of urban sites have emissions higher than 20000 t km^{-2} yr^{-1}, which is only 5% for the suburban sites. For NO_x, 80% of suburban sites show low NO_x emissions of less than 20 t km^{-2} yr^{-1}, and this percentage is also higher

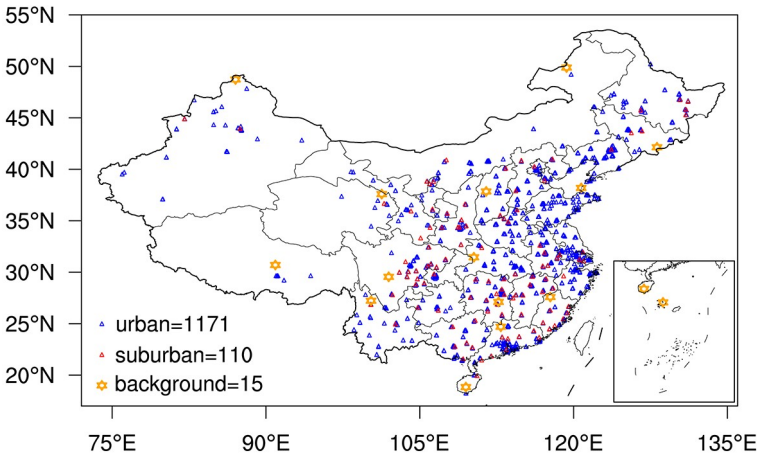

Fig. 1. Distribution of urban (evaluation, blue) and suburban (comparison, red) sites in China. The numbers of sites are shown in the lower-left corner.

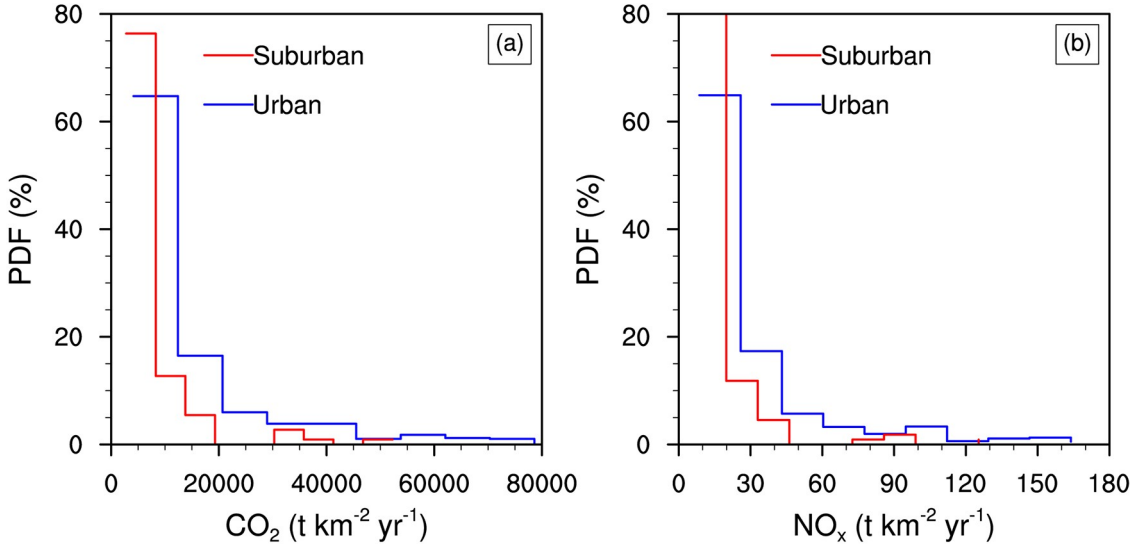

Fig. 2. The PDF of (a) CO_2 and (b) NO_x emissions (units: t km^{-2} yr^{-1}) at urban and suburban sites in 2016.

than that of urban sites (65%). The PDF shows that anthropogenic emissions are generally higher in urban than suburban areas, suggesting different pollution levels between urban and suburban regions.

3.2. *Urban-to-suburban differences of air pollution*

We focus on air pollution in the summer (June–July–August, JJA) and winter (December–January–February, DJF) during 2015–18. Figures 3a–b show the urban and suburban [MDA8] in the four regions. On average, the [MDA8] is higher in summer, with the highest level in BTH and the lowest in PRD (Fig. 3a). In contrast to summer, both the urban and suburban [MDA8] shows a peak in PRD but low values in BTH in winter. The low summertime MDA8 in South China is associated with large quantities of precipitation that wash out precursors in this season (Wang et al., 2017), while the high summertime MDA8 in North China is related to the high temperatures and solar radiation (Zhao et al., 2019).

Figures 3c–d show the urban and suburban [$PM_{2.5}$] in summer and winter, respectively. In summer, [$PM_{2.5}$] is highest in BTH and lowest in PRD, consistent with the distribution of [O_3] in the same season. In winter, the lowest urban and suburban [$PM_{2.5}$] are found in PRD, but the highest values are found in BTH for urban and YRD for suburban areas. Such a winter distribution of [$PM_{2.5}$] generally resembles its summer pattern, except that both the average level and variability are much larger in the cold seasons. The lowest urban and suburban [$PM_{2.5}$] in PRD are related to fewer coal-based industries and favorable meteorological conditions for atmospheric dispersion and dilution (Zhang and Cao, 2015). In comparison, the highest [$PM_{2.5}$] in BTH is associated with the stagnant weather (Chen et al., 2008), high local emissions (Zhang and Cao, 2015), and frequent regional transportation (Huang et al., 2014).

To quantify the urban-to-suburban differences of air pollution, we subtract the average concentration of all sub-

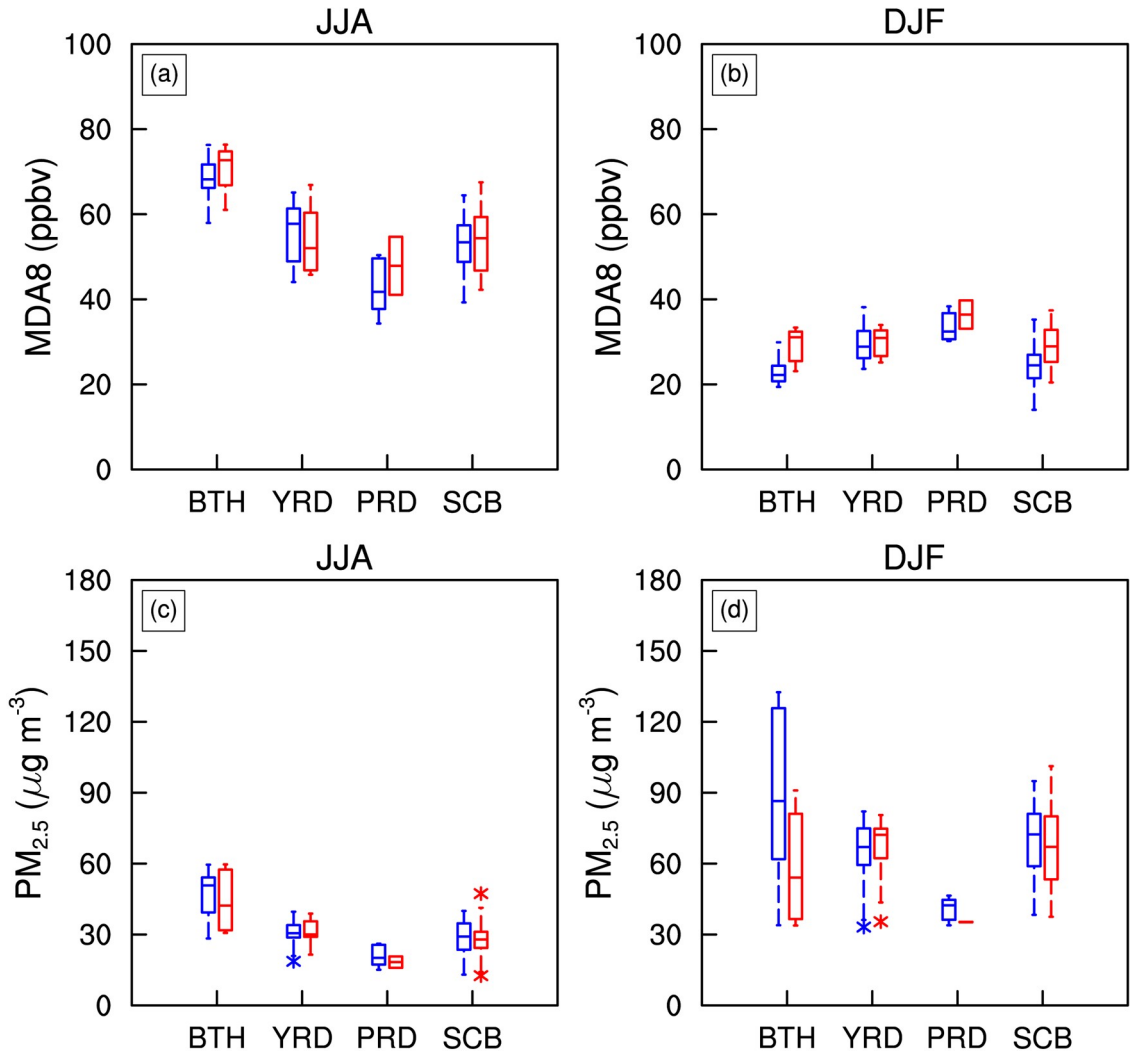

Fig. 3. Comparison of (a, b) MDA8 O_3 (units: ppbv) and (c, d) $PM_{2.5}$ concentrations (units: μg m^{-3}) in (a, c) summer (JJA) and (b, d) winter (DJF) between urban (blue) and suburban (red) sites from 2015 to 2018 in four regions. Each box plot represents the median (middle line), 25th and 75th percentiles (upper and lower boundaries), and the range of summer or winter levels among different sites in a region. The stars show outliers for each region.

urban sites from that of urban sites in the same region and detect the significance of the difference using the Student's *t*-test (significance level: $P < 0.05$) (Fig. 4 and Table S1). The Δ[MDA8] is negative for almost all regions, indicating that the suburban [MDA8] is higher than that in urban areas, except for YRD in summer (Δ[MDA8] = 2.7 ppbv). For YRD, high emissions of biogenic and anthropogenic VOCs (Liu et al., 2018) and the substantial NO_x reductions (He et al., 2017; Song et al., 2017) convert a VOC-limited regime to a mixed sensitive environment (Jin and Holloway, 2015), leading to a positive (though nonsignificant) urban-to-suburban Δ[MDA8] via the higher urban NO_2 level (Fig. 4c). In contrast to MDA8, the Δ[$PM_{2.5}$] is generally positive in the four regions (Fig. 4b), suggesting that concentrations of urban $PM_{2.5}$ are usually higher than in suburban areas. Negative but nonsignificant Δ[$PM_{2.5}$] values of −0.04 (summer) and −0.6 μg m^{-3} (winter) are found in YRD.

We calculate the urban-to-suburban differences in the NO_2, SO_2 and NO_2 to O_3 ratio, and the $PM_{2.5}$ to PM_{10} ratio (Figs. 4c–f), to determine the possible reasons for the differences of MDA8 and $PM_{2.5}$. It should be noted that the [MDA8] between urban and suburban areas is significantly different only in BTH (−7.0 ppbv) and SCB (−6.3 ppbv) during winter. In these two regions, the urban NO_2 concentrations are significantly higher than the suburban ones by 6.0–10.0 ppbv (Fig. 4c). As O_3 can be titrated by NO via the reaction $NO + O_3 \rightarrow NO_2 + O_2$ (Sillman, 1999; Murphy et al., 2007), the higher level of NO_2 in urban areas indicates strong conversions from NO to NO_2 (Tong et al., 2017), leading to higher O_3 loss and lower [MDA8] in urban areas (Fig. 4a). This is also evidenced by the highest NO_2 to O_3 ratios over urban sites in BTH and SCB (Fig. 4e). In BTH, the urban [$PM_{2.5}$] during winter is significantly higher than that observed in suburbs (32.7 μg m^{-3}), which is mainly due to secondary production. Different from the three other regions, Δ[SO_2] and Δ[NO_2] in BTH are much higher (Figs.

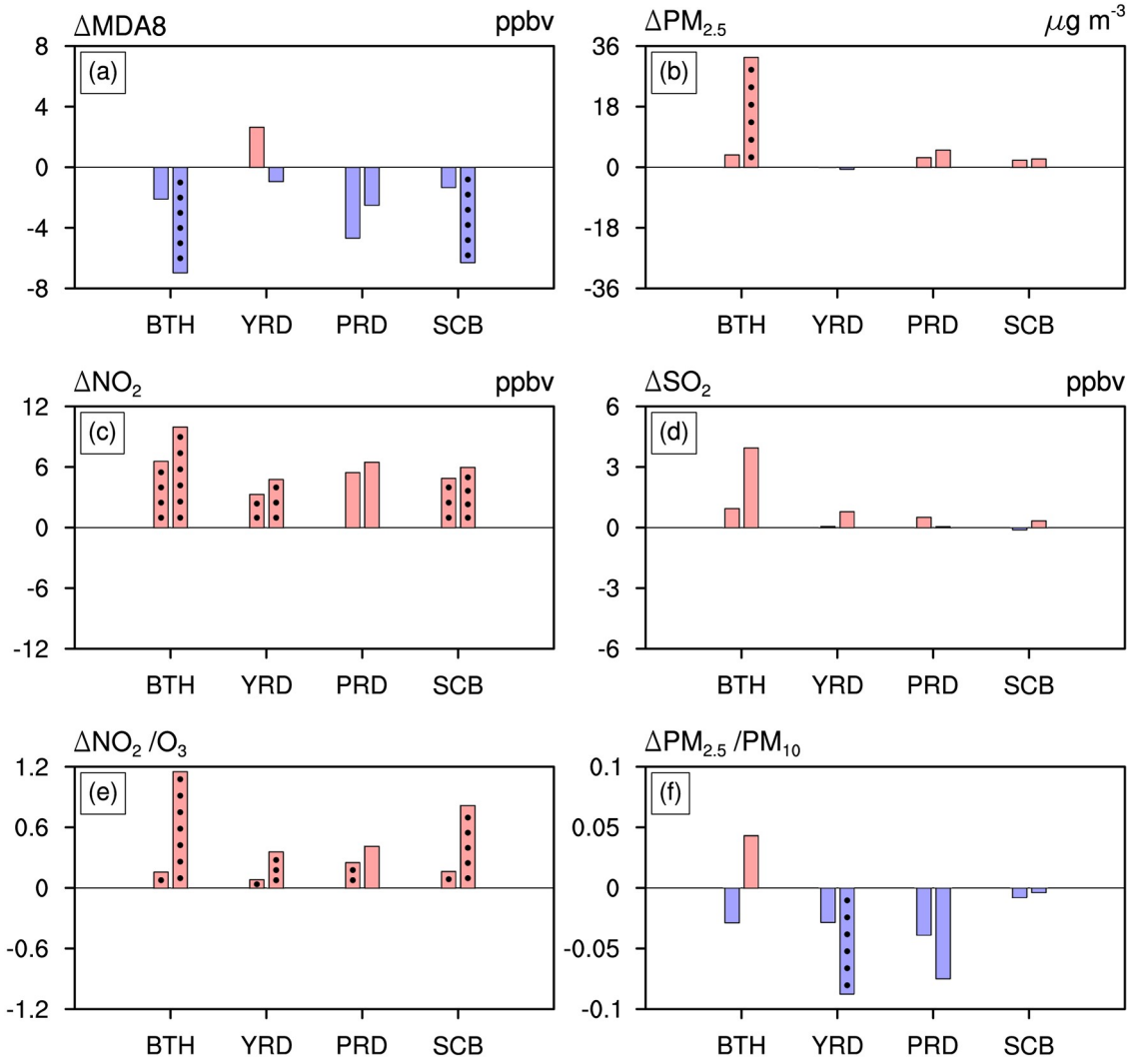

Fig. 4. The urban-to-suburban differences in concentrations of (a) MDA8 O_3 (units: ppbv), (b) $PM_{2.5}$ (units: μg m^{-3}), (c) NO_2 (units: ppbv), (d) SO_2 (units: ppbv), (e) NO_2 to O_3 ratio, and (f) $PM_{2.5}$ to PM_{10} ratio, in summer (left-hand bars) and winter (right-hand bars), from 2015 to 2018, in four regions. The black dots denote that the difference is statistically significant $P < 0.05$).

4c–d). Furthermore, the $PM_{2.5}$ to PM_{10} ratio over urban sites is larger than in the suburbs (Fig. 4f), suggesting that secondary formation of fine particles contributes more than primary emissions in the urban areas of BTH.

3.3. *Temporal variations of urban-to-suburban differences*

We quantify the diurnal, weekly, seasonal, and interannual variations of the urban-to-suburban differences of O_3 and $PM_{2.5}$ in the four regions (Fig. 5). The hourly $[O_3]$ is used to study the diurnal variation (Fig. 5a). During daytime, the absolute $\Delta[O_3]$ peaks at 0800 LST (local standard time) in most sub-regions, especially for BTH (−8.7 ppbv) and SCB (−5.5 ppbv), likely due to high NO_x emissions from traffic in the rush hour (Dominguez-Lopez et al., 2014). Traffic emissions are also an important driver for $\Delta[PM_{2.5}]$, the peak of which (21.0 μg m^{-3}) is found at 0800 LST in BTH (Fig. 5e, Table S2). In addition, high values of $\Delta[PM_{2.5}]$ may be caused by relatively low boundary-layer heights (Zhang and Cao, 2015) and weaker turbulence (Miao et al., 2016) in urban areas.

We use the daily $[O_3]$ to study the weekly variations of urban-to-suburban differences (Fig. 5b). The ozone weekend effect (OWE) indicates that the daily mean $[O_3]$ (not [MDA8]) is lower on weekdays than weekends owing to lower anthropogenic NO_x emissions at weekends (Tong et al., 2017). However, our results do not find the OWE in all sub-regions, except for the urban areas in YRD and PRD, where the differences between weekday and weekend $[O_3]$ are nonsignificant (Table S3). For suburban areas, a positive $\Delta[O_3]$ between weekdays and weekends is found, with a maximum difference of 6.8 ppbv in YRD. No significant differences of $\Delta[PM_{2.5}]$ are found between weekdays and weekends (Fig. 5f).

Both the Δ[MDA8] (Fig. 5c) and $\Delta[PM_{2.5}]$ (Fig. 5g) show seasonal variation in the four regions. The year-round Δ[MDA8] is generally negative, except in spring and summer in YRD, which may be related to the nonlinear relationship of precursor emissions (Liu et al., 2018). In contrast, most $\Delta[PM_{2.5}]$ values are positive, except for YRD. The absolute values of Δ[MDA8] and $\Delta[PM_{2.5}]$ usually show peaks in winter and lows in summer, when there are more rainy days in BTH and SCB.

We further examine the interannual variations of Δ[MDA8] (Fig. 5d) and $\Delta[PM_{2.5}]$ (Fig. 5h). The absolute Δ[MDA8] exhibits a decreasing trend over BTH and PRD but an increasing trend in SCB during 2015–18. For YRD, the value of Δ[MDA8] shifts from positive to negative after the year 2016. The values of $\Delta[PM_{2.5}]$ generally decrease in all regions. In YRD, the $\Delta[PM_{2.5}]$ is positive during 2015–16, but has become negative since 2017, though its magnitude is close to zero (Table S2). On an annual mean basis, the suburban [MDA8] is higher than the urban value by 3.7 ppbv in BTH, 3.5 ppbv in PRD, and 3.8 ppbv in SCB. In comparison, the $[PM_{2.5}]$ in suburban areas is lower than the urban value by 15.8 μg m^{-3} in BTH, 3.5 μg m^{-3} in PRD, and

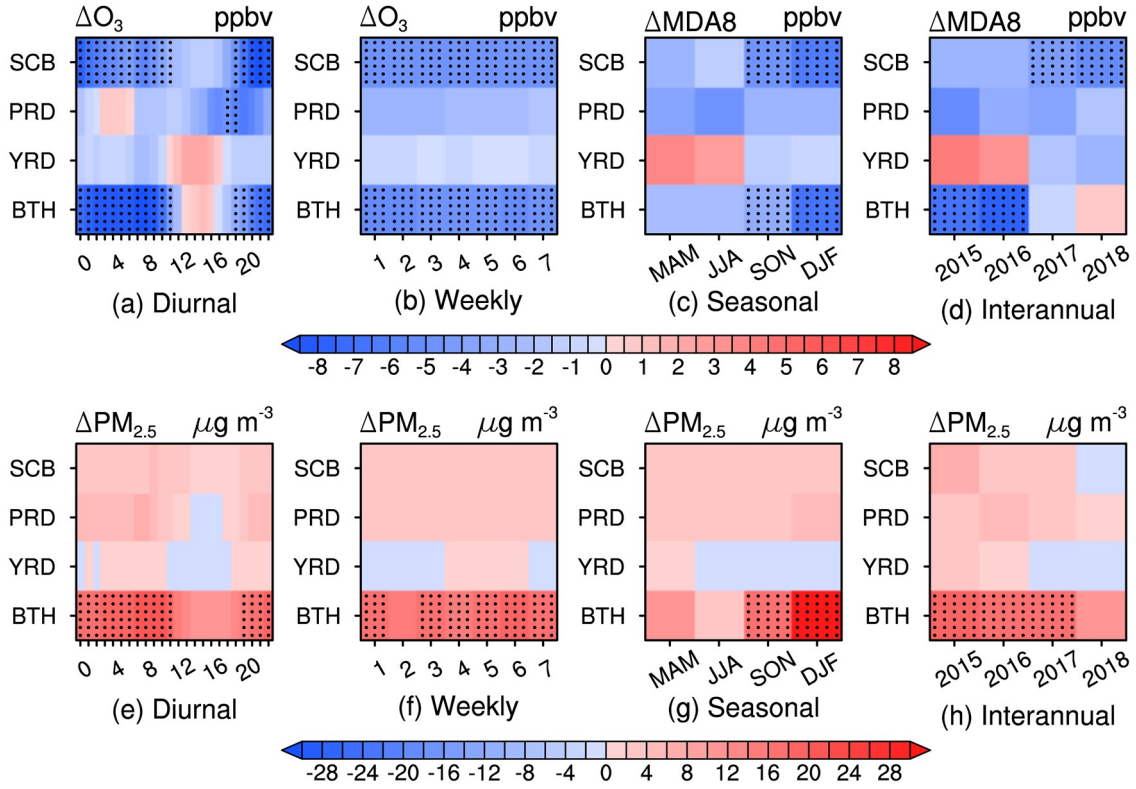

Fig. 5. (a, e) Diurnal, (b, f) weekly, (c, g) seasonal and (d, h) interannual variations of urban-to-suburban differences of (a–d) O_3 (units: ppbv) and (e–h) $PM_{2.5}$ (units: μg m^{-3}) from 2015 to 2018 in four regions. The black dots denote that the difference is statistically significant ($P < 0.05$). The values are shown in Table S2.

2.4 μg m^{-3} in SCB.

The variations of urban-to-nonurban differences of air pollution are related to the ambient pollution levels. Figure 6 illustrates the variations of Δ[MDA8] at different ranges of urban [MDA8] on a daily basis from 2015 to 2018. In BTH and SCB, the median Δ[MDA8] shifts from a negative to positive value with an elevated urban [MDA8], suggesting that the increase of [MDA8] at urban sites is faster than at suburban sites. In summer, the urban [MDA8] can be either high (e.g., sunny days) or low (e.g., rainy days) on different days. As a result, the positive and negative Δ[MDA8] values may offset each other, leading to a limited average Δ[MDA8] (Fig. 4a). In winter, the urban [MDA8] is usually low, leading to a strong and negative Δ[MDA8] in these sub-regions (Fig. 5c). In comparison, the Δ[$PM_{2.5}$] changes from near zero to more positive values with the increase of urban [$PM_{2.5}$] in all four regions (Fig. 7). As the [$PM_{2.5}$] rises, there is an overall increasing trend and variability of Δ[$PM_{2.5}$]. This suggests that the [$PM_{2.5}$] in urban areas grows faster compared to in suburban areas during pollution episodes, and the Δ[$PM_{2.5}$] is linearly dependent on the urban [$PM_{2.5}$]. As a result, the Δ[$PM_{2.5}$] shows large positive values during winter season, when the urban [$PM_{2.5}$] is usually high (Fig. 4b).

3.4. *Comparison of air pollutants over urban, suburban and background sites*

In total, there are 10 background sites in the central-east-

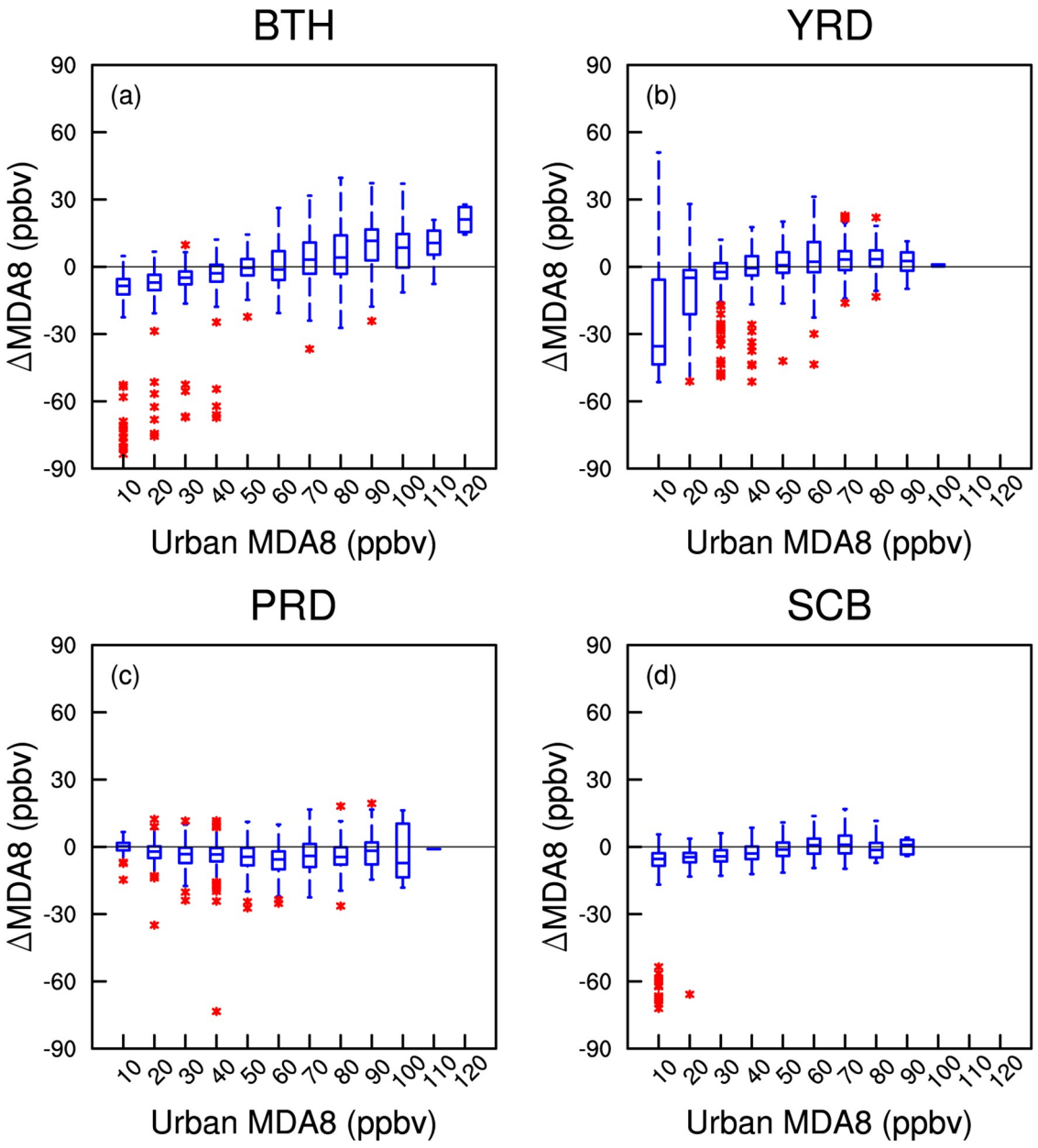

Fig. 6. Changes of daily Δ[MDA8] (units: ppbv) with different levels of urban [MDA8] (units: ppbv) from 2015 to 2018. The red stars show outliers for each interval of [MDA8].

ern China region (18°–43°N, 100°–125°E), the number of which is much smaller than that of urban and suburban sites. Here, we compare the annual mean [MDA8] and [$PM_{2.5}$] at these background sites to the nearby urban and suburban sites within a 2° × 2° grid cell (Table 1 and Table S4). On average, the background [MDA8] (37.8–55.0 ppbv) is higher by 12% than in urban areas, and by 5% than in suburban areas. We find better correlations of [MDA8] between the background and suburban sites (R = 0.8) than those between the background and urban sites (R = 0.4) (Fig. 8). In contrast, the [$PM_{2.5}$] over background sites (6.7–33 μg m^{-3}) is lower by 45% than in urban areas, and by 30% than in suburban areas (Fig. 9), with a higher correlation coefficient between background and suburban sites (R = 0.8). As for the regression fits, suburban values are closer to the background concentrations for O_3, consistent with the findings in previous studies (Tong et al., 2017; Huang et al., 2018).

We further calculate the Δ[MDA8] and Δ[$PM_{2.5}$] for summer (JJA) and winter (November–December, ND) between urban and background sites in 2017. Results show that the absolute urban-to-background (urban minus background) differences of [MDA8] and [$PM_{2.5}$] are much larger in winter than summer (Fig. 10), consistent with the seasonal variations of urban-to-suburban differences (Fig. 4). In summer, a moderate contrast of air pollution (−5.1 to 6.8 ppbv for Δ[MDA8] and −0.1 to 22.5 μg m^{-3} for Δ[$PM_{2.5}$]) is found between urban and background sites (Table S5). However, such a contrast is much larger and more significant in winter (−22.2 to 5.5 ppbv for Δ[MDA8] and 3.1 to 82.3 μg m^{-3}

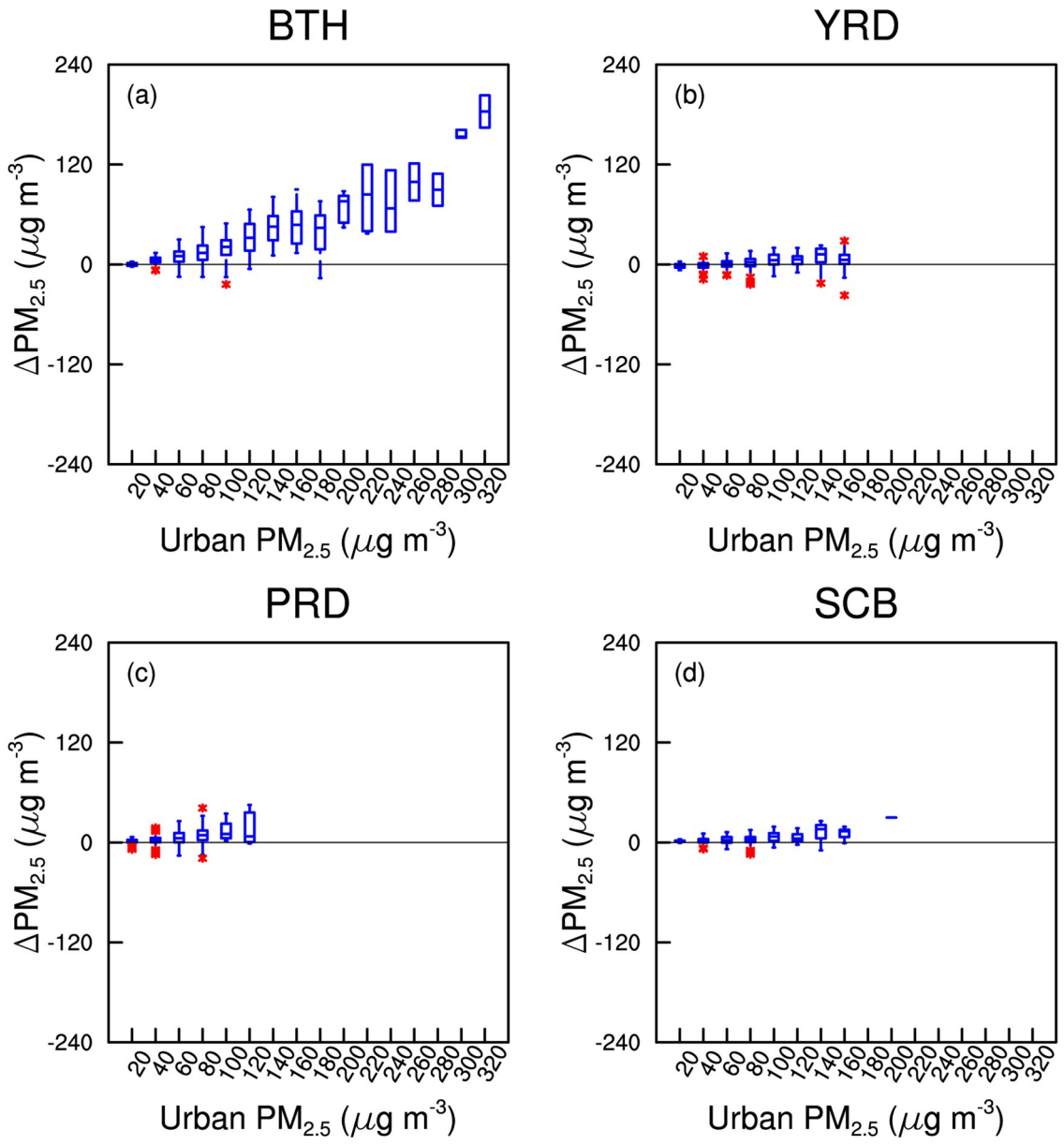

Fig. 7. Changes of daily Δ[$PM_{2.5}$] (units: μg m^{-3}) with different levels of urban [$PM_{2.5}$] (units: μg m^{-3}) from 2015 to 2018. The red stars show outliers for each interval of [$PM_{2.5}$].

Table 1. Information on 10 background sites in central-eastern China (18°–43°N, 100°–125°E), including name, annual mean [MDA8] (ppbv), and [$PM_{2.5}$] (μg m^{-3}), and the range of concentrations for nearby urban and suburban sites within a 2° × 2° grid cell. The numbers and distances of the nearby sites are shown in Table S4.

Site ID	Name	MDA8	Urban MDA8	Suburban MDA8	$PM_{2.5}$	Urban $PM_{2.5}$	Suburban $PM_{2.5}$
1	Pangquangou, Shanxi	51.2	37.8–43.0	–	19.7	53.0–74.7	–
2	Wuyishan, Fujian	50.8	37.9–44.5	41.4–42.6	17.3	22.7–46.0	32.7–41.0
3	Changdao, Shandong	38.8	42.8–54.8	–	33.0	29.5–47.3	–
4	Shenlongjia, Hubei	47.0	38.7	42.6	9.2	56.5	31.5
5	Hengshan, Hunan	48.7	34.0–43.9	39.5–45.3	23.5	39.1–60.0	43.3–47.7
6	Nanling, Guangdong	46.9	43.0–46.8	–	13.3	34.8–42.9	–
7	Wuzhishan, Hainan	37.8	31.5–33.8	–	11.2	14.6–15.6	–
8	Hailuogou, Sichuan	39.3	–	–	6.7	–	–
9	Lijiang, Yunnan	39.0	33.5–42.0	40.2	7.6	11.5–15.2	17.1
10	Menyuan, Qinghai	55.0	46.5–51.3	52.4	12.7	25.7–39.7	42.5

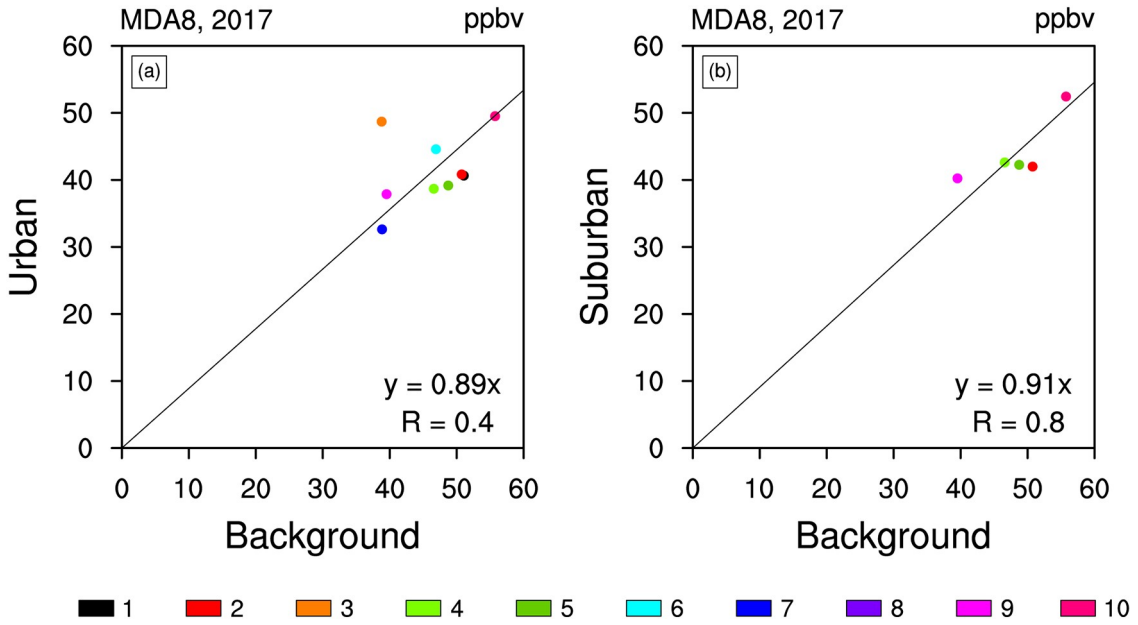

Fig. 8. Comparison of annual mean MDA8 O_3 concentrations (units: ppbv) at 10 background sites to nearby urban and suburban sites within a 2° × 2° grid cell in central-eastern China (18°–43°N, 100°–125°E) in 2017. The numbers from 1 to 10 correspond to those in Table 1.

for Δ[$PM_{2.5}$]). Exceptions of positive Δ[MDA8] are found at sites 4, 5, 6 and 9 in JJA (Fig. 10a), suggesting that the sign of urban-to-background Δ[O_3] is not uniform on the country level during summer.

4. Discussion and conclusions

We compare our results with previous studies and find both agreements and differences. Studies have shown that diurnal variations of urban [O_3] are opposite to those of NO_x emissions, which peak at 0800 LST during the rush hour (Zheng et al., 2010; Al-Rashidi et al., 2018). Such variations may result in negative peaks of Δ[O_3] within a diurnal circle, consistent with our findings (Fig. 5a). We do not find an OWE in BTH (Table S3), though some weekend effects in Beijing have been reported by Wang et al.(2015). The positive Δ[MDA8] during spring and summer in YRD is quite different from those over the three other regions (Fig. 5c), likely because of regionally high emissions of both biogenic and anthropogenic VOCs (Liu et al., 2018) and the substantial NO_x reductions (He et al., 2017; Song et al., 2017) transform a VOC-limited regime to a mixed sensitive environment over YRD (Jin and Holloway, 2015) and result in the increase in urban O_3 (Wang et al., 2019). In terms of interannual variation, Huang et al.(2018) found that the urban [O_3] in Shenzhen, a city in PRD, increased faster than its nonurban counterpart during 2012–17, leading to a decline in the absolute Δ[MDA8]. A similar trend is also present in our analyses for the whole PRD domain during 2015–18 (Fig. 5d).

For $PM_{2.5}$, Zheng et al. (2018) examined $PM_{2.5}$ in Beijing during 2012–16 and found two peaks of Δ[$PM_{2.5}$],

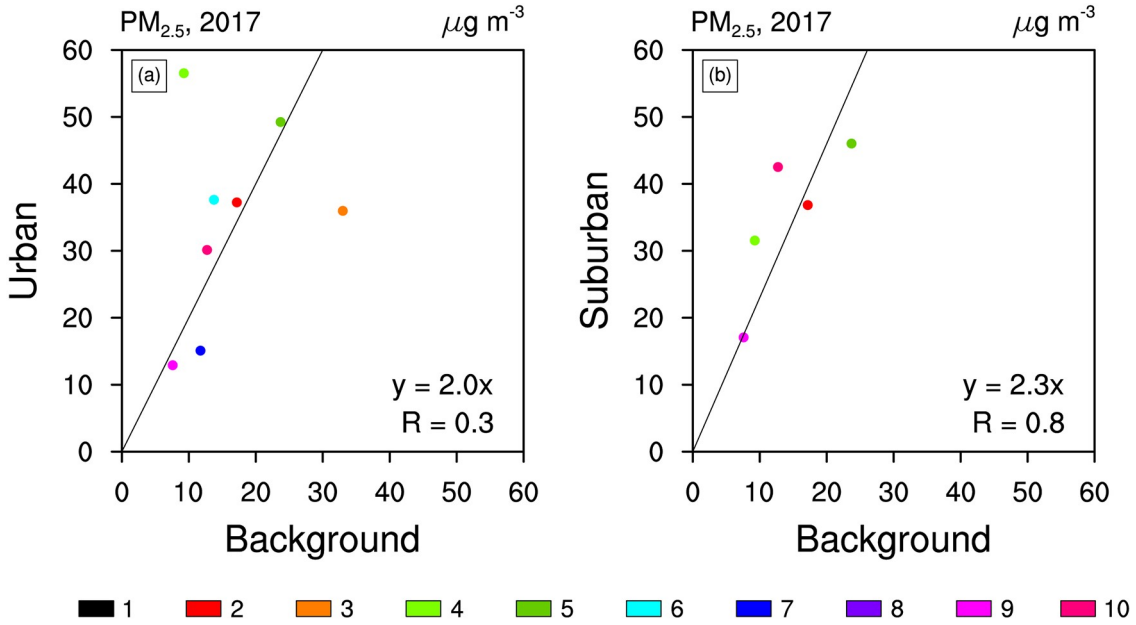

Fig. 9. Comparison of annual mean $PM_{2.5}$ concentrations (units: μg m^{-3}) at 10 background sites to nearby urban and suburban sites within a 2° × 2° grid cell in central-eastern China (18°–43°N, 100°–125°E) in 2017. Data of site 1 is outside the axis range.

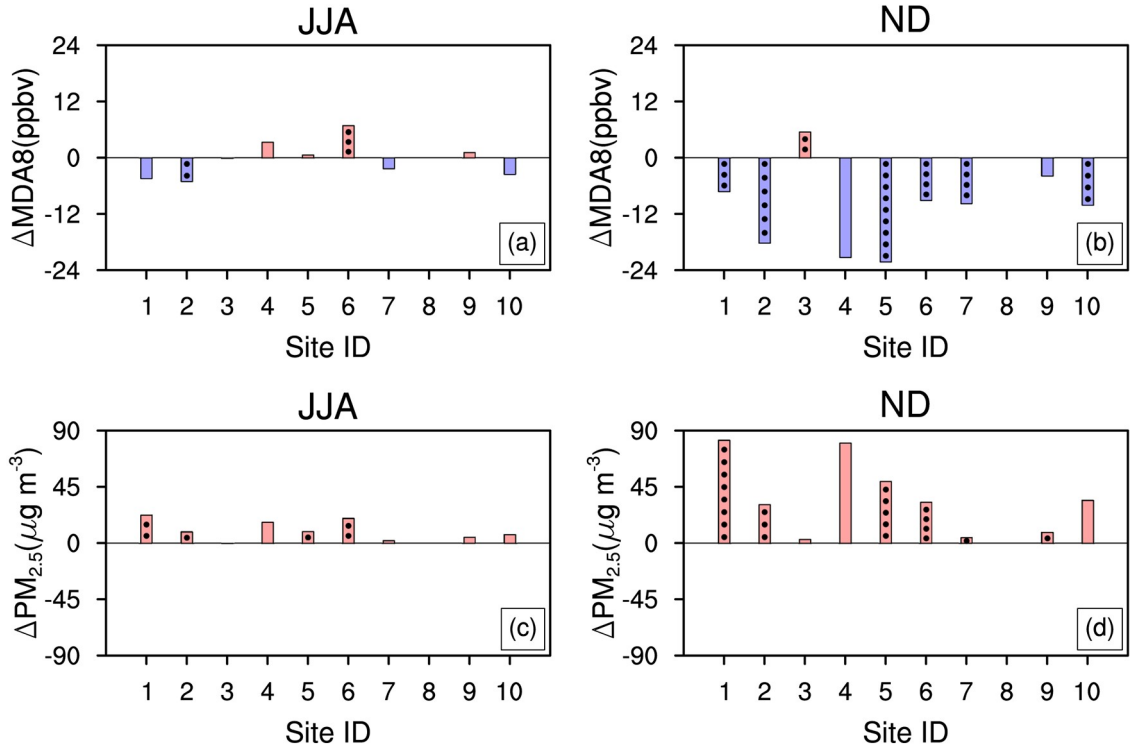

Fig. 10. The urban-to-background differences in concentrations of (a, b) MDA8 O_3 (units: ppbv) and (c, d) $PM_{2.5}$ (units: μg m^{-3}) in (a, c) summer (JJA) and (b, d) winter (ND) of 2017 between 10 background sites and their surrounding urban sites within a 2° × 2° grid cell. The numbers from 1 to 10 correspond to those in Table 1. The black dots denote that the difference is statistically significant ($P < 0.05$).

at 1100 LST and 2300 LST respectively. The first occurs three hours later than our results for 2015–18. At the seasonal scale, the absolute Δ[$PM_{2.5}$] was found to be larger in winter than in summer, because of urban emissions from heating in the cold season, which is consistent with our results (Fig. 5g). The year-to-year $PM_{2.5}$ level is decreasing owing to the effective emissions regulations imposed during the past decade (Lei et al., 2011; Lu et al., 2011; Zhao et al.,

2013). Such a trend is more significant in urban regions than in nonurban areas (Lin et al., 2018), explaining the downward trends of $\Delta[PM_{2.5}]$ in BTH, YRD, PRD, and SCB, especially after the year 2016 (Fig. 5h).

It is important to acknowledge that there are some uncertainties in our analyses. One major source of uncertainty originates from the classification of urban and suburban sites based on the official documents of the MEE. It has been more than a decade since these suburban sites were set up in 2007. During this period, urbanization has been increasing rapidly, which may have turned some suburban sites, which were originally built far away from urban centers and pollutant sources, into urban sites (Yan et al., 2010; Yang et al., 2013). This may result in reduced differences of air pollutants like O_3 and $PM_{2.5}$ between urban and suburban areas from year to year (Figs. 5d and h). Furthermore, the number of suburban sites built by the CNEMC is far fewer than urban ones, leading to biases in interpolations and comparisons. After trying to use other information, such as administrative divisions and satellite-based land-cover types/built-up percentages, we found that the classification based on the MEE definition is the most effective way to distinguish urban and suburban sites. It is still valid for our study period because urban emissions with this classification are larger than the suburban emissions for 2016 (Fig. 2). In China, the paucity of background observation sites is a limitation for research into the effects of O_3 on ecosystems, as background information is needed for comprehensive validations of modeled O_3 (Yue et al., 2017). We find that the urban-to-background differences of O_3 are not significantly different by a large majority during summer, suggesting that data of urban sites from the CNEMC network can be directly used to study ecological effects of O_3 that are also mostly concentrated in summer.

In this study, we analyze the differences of O_3 and $PM_{2.5}$ between urban and suburban areas in four megacity clusters (BTH, YRD, PRD and SCB) at different time scales (diurnal, weekly, seasonal and interannual). We find that the differences vary in time and space, but the pattern whereby the suburban [MDA8] is higher and the urban $[PM_{2.5}]$ is higher, dominates. However, obvious seasonal variations are observed. Both the urban-to-suburban and urban-to-background pollution shows a more significant contrast in winter (Figs. 4 and 10). According to national statistics (http://www.stats.gov.cn/), the total urban area was 2×10^5 km^2 in China in 2018, which was only 2% of the national total area. As a result, air quality monitoring sites built mainly in urban areas can reasonably capture country-level pollution in summer but may overestimate the national average $[PM_{2.5}]$, and underestimate the [MDA8] in winter.

Acknowledgements. This work was jointly supported by the National Key Research and Development Program of China (Grant No. 2019YFA0606802) and the National Natural Science Foundation of China (Grant No. 41975155).

Electronic supplementary material: Supplementary material is available in the online version of this article at https//doi.org/10.1007/s00376-020-0054-2.

REFERENCES

Al-Rashidi, M. S., M. F. Yassin, N. S. Alhajeri, and M. J. Malek, 2018: Gaseous air pollution background estimation in urban, suburban, and rural environments. *Arabian Journal of Geosciences*, **11**, 59, https://doi.org/10.1007/s12517-017-3369-2.

An, J. L., J. N. Zou, J. X. Wang, X. Lin, and B. Zhu, 2015: Differences in ozone photochemical characteristics between the megacity Nanjing and its suburban surroundings, Yangtze River Delta, China. *Environmental Science and Pollution Research*, **22**, 19 607–19 617, https://doi.org/10.1007/s11356-015-5177-0.

Banan, N., M. T. Latif, L. Juneng, and F. Ahamad, 2013: Characteristics of surface ozone concentrations at stations with different backgrounds in the Malaysian Peninsula. *Aerosol and Air Quality Research*, **13**, 1090–1106, https://doi.org/10.4209/aaqr.2012.09.0259.

Barmpadimos, I., M. Nufer, D. C. Oderbolz, J. Keller, S. Aksoyoglu, C. Hueglin, U. Baltensperger, and A. S. H. Prévôt, 2011: The weekly cycle of ambient concentrations and traffic emissions of coarse (PM_{10}-$PM_{2.5}$) atmospheric particles. *Atmos. Environ.*, **45**, 4580–4590, https://doi.org/10.1016/j.atmosenv.2011.05.068.

Bravo, M. A., R. Anthopolos, M. L. Bell, and M. L. Miranda, 2016: Racial isolation and exposure to airborne particulate matter and ozone in understudied US populations: Environmental justice applications of downscaled numerical model output. *Environment International*, **92–93**, 247–255, https://doi.org/10.1016/j.envint.2016.04.008.

Chen, Z. H., S. Y. Cheng, J. B. Li, X. R. Guo, W. H. Wang, and D. S. Chen, 2008: Relationship between atmospheric pollution processes and synoptic pressure patterns in northern China. *Atmos. Environ.*, **42**, 6078–6087, https://doi.org/10.1016/j.atmosenv.2008.03.043.

Chow, J. C., 2006: Introduction to the A&WMA 2006 Critical Review - Health effects of fine particulate air pollution: Lines that connect. *Journal of the Air & Waste Management Association*, **56**, 707–708, https://doi.org/10.1080/10473289.2006.10464484.

Dominguez-Lopez, D., J. A. Adame, M. A. Hernández-Ceballos, F. Vaca, B. A. De La Morena, and J. P. Bolívar, 2014: Spatial and temporal variation of surface ozone, NO and NO_2 at urban, suburban, rural and industrial sites in the southwest of the Iberian Peninsula. *Environmental Monitoring and Assessment*, **186**, 5337–5351, https://doi.org/10.1007/s10661-014-3783-9.

Dueñas, C., M. C. Fernández, S. Cañete, J. Carretero, and E. Liger, 2004: Analyses of ozone in urban and rural sites in Málaga (Spain). *Chemosphere*, **56**, 631–639, https://doi.org/

10.1016/j.chemosphere.2004.04.013.

Ge, B. Z., X. B. Xu, W. L. Lin, J. Li, and Z. F. Wang, 2012: Impact of the regional transport of urban Beijing pollutants on downwind areas in summer: Ozone production efficiency analysis. *Tellus B: Chemical and Physical Meteorology*, **64**, 17348, https://doi.org/10.3402/tellusb.v64i0.17348.

George, K., L. H. Ziska, J. A. Bunce, and B. Quebedeaux, 2007: Elevated atmospheric CO_2 concentration and temperature across an urban-rural transect. *Atmos. Environ.*, **41**, 7654–7665, https://doi.org/10.1016/j.atmosenv.2007.08.018.

Gregg, J. W., C. G. Jones, and T. E. Dawson, 2003: Urbanization effects on tree growth in the vicinity of New York City. *Nature*, **424**, 183–187, https://doi.org/10.1038/nature01728.

Han, S. Q., M. Zhang, C. S. Zhao, X. Q. Lu, L. Ran, M. Han, P. Y. Li, and X. J. Li, 2013: Differences in ozone photochemical characteristics between the megacity Tianjin and its rural surroundings. *Atmos. Environ.*, **79**, 209–216, https://doi.org/10.1016/j.atmosenv.2013.06.045.

He, J. J., and Coauthors, 2017: Air pollution characteristics and their relation to meteorological conditions during 2014-2015 in major Chinese cities. *Environmental Pollution*, **223**, 484–496, https://doi.org/10.1016/j.envpol.2017.01.050.

Huang, D., Q. L. Li, X. X. Wang, G. X. Li, L. Q. Sun, B. He, L. Zhang, and C. S. Zhang, 2018: Characteristics and trends of ambient ozone and nitrogen oxides at urban, suburban, and rural sites from 2011 to 2017 in Shenzhen, China. *Sustainability*, **10**, 4530, https://doi.org/10.3390/su10124530.

Huang, R. J., and Coauthors, 2014: High secondary aerosol contribution to particulate pollution during haze events in China. *Nature*, **514**, 218–222, https://doi.org/10.1038/nature13774.

Jin, X. M. and T. Holloway, 2015: Spatial and temporal variability of ozone sensitivity over China observed from the Ozone Monitoring Instrument. *J. Geophys. Res.*, **120**, 7229–7246, https://doi.org/10.1002/2015jd023250.

Lei, Y., Q. Zhang, K. B. He, and D. G. Streets, 2011: Primary anthropogenic aerosol emission trends for China, 1990-2005. *Atmospheric Chemistry and Physics*, **11**, 931–954, https://doi.org/10.5194/acp-11-931-2011.

Li, K., D. J. Jacob, H. Liao, L. Shen, Q. Zhang, and K. H. Bates, 2019: Anthropogenic drivers of 2013-2017 trends in summer surface ozone in China. *Proceedings of the National Academy of Sciences of the United States of America*, **116**, 422–427, https://doi.org/10.1073/pnas.1812168116.

Lin, C. Q., A. K. H. Lau, Y. Li, J. C. H. Fung, C. C. Li, X. C. Lu, and Z. Y. Li, 2018: Difference in $PM_{2.5}$ variations between urban and rural areas over eastern China from 2001 to 2015. *Atmosphere*, **9**, 312, https://doi.org/10.3390/atmos9080312.

Liu, Y., and Coauthors, 2018: Estimation of biogenic VOC emissions and its impact on ozone formation over the Yangtze River Delta region, China. *Atmos. Environ.*, **186**, 113–128, https://doi.org/10.1016/j.atmosenv.2018.05.027.

Lu, X., and Coauthors, 2018: Severe Surface Ozone Pollution in China: A Global Perspective. *Environmental Science & Technology Letters*, **5**, 487–494, https://doi.org/10.1021/acs.estlett.8b00366.

Lu, Z., Q. Zhang, and D. G. Streets, 2011: Sulfur dioxide and primary carbonaceous aerosol emissions in China and India, 1996-2010. *Atmospheric Chemistry and Physics*, **11**, 9839–9864, https://doi.org/10.5194/acp-11-9839-2011.

Miao, Y. C., S. H. Liu, Y. J. Zheng, and S. Wang, 2016: Modeling the feedback between aerosol and boundary layer processes: A case study in Beijing, China. *Environmental Science and Pollution Research*, **23**, 3342–3357, https://doi.org/10.1007/s11356-015-5562-8.

Mills, G., and Coauthors, 2018: Tropospheric Ozone Assessment Report: Present-day tropospheric ozone distribution and trends relevant to vegetation. *Elementa-Science of the Anthropocene*, **6**, 47, https://doi.org/10.1525/elementa.302.

Murphy, J. G., D. A. Day, P. A. Cleary, P. J. Wooldridge, D. B. Millet, A. H. Goldstein, and R. C. Cohen, 2007: The weekend effect within and downwind of Sacramento - Part 1: Observations of ozone, nitrogen oxides, and VOC reactivity. *Atmospheric Chemistry and Physics*, **7**, 5327–5339, https://doi.org/10.5194/acp-7-5327-2007.

Pataki, D. E., and Coauthors, 2006: Urban ecosystems and the North American carbon cycle. *Global Change Biology*, **12**, 2092–2102, https://doi.org/10.1111/j.1365-2486.2006.01242.x.

Pope III, C. A., and D. W. Dockery, 2013: Air pollution and life expectancy in China and beyond. *Proceedings of the National Academy of Sciences of the United States of America*, **110**, 12 861–12 862, https://doi.org/10.1073/pnas.1310925110.

Putaud, J. P., and Coauthors, 2004: European aerosol phenomenology—2: Chemical characteristics of particulate matter at kerbside, urban, rural and background sites in Europe. *Atmos. Environ.*, **38**, 2579–2595, https://doi.org/10.1016/j.atmosenv.2004.01.041.

Qu, Y. W., and Coauthors, 2018: Influence of atmospheric particulate matter on ozone in Nanjing, China: Observational study and mechanistic analysis. *Adv. Atmos. Sci.*, **35**, 1381–1395, https://doi.org/10.1007/s00376-018-8027-4.

Shu, L., T. J. Wang, M. Xie, M. M. Li, M. Zhao, M. Zhang, and X. Y. Zhao, 2019: Episode study of fine particle and ozone during the CAPUM-YRD over Yangtze River Delta of China: Characteristics and source attribution. *Atmos. Environ.*, **203**, 87–101, https://doi.org/10.1016/j.atmosenv.2019.01.044.

Sillman, S., 1999: The relation between ozone, NO_x and hydrocarbons in urban and polluted rural environments. *Atmos. Environ.*, **33**, 1821–1845, https://doi.org/10.1016/s1352-2310(98)00345-8.

Sillman, S., P. J. Samson, and J. M. Masters, 1993: Ozone production in urban plumes transported over water: Photochemical model and case studies in the northeastern and midwestern United States. *J. Geophys. Res.*, **98**, 12 687–12 699, https://doi.org/10.1029/93JD00159.

Song, C. B., and Coauthors, 2017: Air pollution in China: Status and spatiotemporal variations. *Environmental Pollution*, **227**, 334–347, https://doi.org/10.1016/j.envpol.2017.04.075.

Tong, L., and Coauthors, 2017: Characteristics of surface ozone and nitrogen oxides at urban, suburban and rural sites in Ningbo, China. *Atmospheric Research*, **187**, 57–68, https://doi.org/10.1016/j.atmosres.2016.12.006.

Turner, M. C., and Coauthors, 2016: Long-term ozone exposure and mortality in a large prospective study. *American Journal of Respiratory and Critical Care Medicine*, **193**, 1134–1142, https://doi.org/10.1164/rccm.201508-1633OC.

Wang, N., X. P. Lyu, X. J. Deng, X. Huang, F. Jiang, and A. J. Ding, 2019: Aggravating O_3 pollution due to NO_x emission control in eastern China. *Science of The Total Environment*, **677**, 732–744, https://doi.org/10.1016/j.scitotenv.2019.04.388.

Wang, T., L. K. Xue, P. Brimblecombe, Y. F. Lam, L. Li, and L.

Zhang, 2017: Ozone pollution in China: A review of concentrations, meteorological influences, chemical precursors, and effects. *Science of the Total Environment*, **575**, 1582–1596, https://doi.org/10.1016/j.scitotenv.2016.10.081.

Wang, Z. S., and Coauthors, 2015: Ground-level ozone in urban Beijing over a 1-year period: Temporal variations and relationship to atmospheric oxidation. *Atmospheric Research*, **164–165**, 110–117, https://doi.org/10.1016/j.atmosres.2015.05.005.

Xing, J., S. X. Wang, C. Jang, Y. Zhu, and J. M. Hao, 2011: Nonlinear response of ozone to precursor emission changes in China: A modeling study using response surface methodology. *Atmospheric Chemistry and Physics*, **11**, 5027–5044, https://doi.org/10.5194/acp-11-5027-2011.

Xu, W., Q. H. Wu, X. J. Liu, A. H. Tang, A. J. Dore, and M. Heal, 2016: Characteristics of ammonia, acid gases, and $PM_{2.5}$ for three typical land-use types in the North China Plain. *Environmental Science and Pollution Research*, **23**, 1158–1172, https://doi.org/10.1007/s11356-015-5648-3.

Xue, L. K., and Coauthors, 2014: Ground-level ozone in four Chinese cities: Precursors, regional transport and heterogeneous processes. *Atmospheric Chemistry and Physics*, **14**, 13 175–13 188, https://doi.org/10.5194/acp-14-13175-2014.

Yan, Z. W., Z. Li, Q. X. Li, and P. Jones, 2010: Effects of site change and urbanisation in the Beijing temperature series 1977-2006. *International Journal of Climatology*, **30**, 1226–1234, https://doi.org/10.1002/joc.1971.

Yang, P., G. Y. Ren, and W. D. Liu, 2013: Spatial and Temporal Characteristics of Beijing Urban Heat Island Intensity. *J. Appl. Meteorol. Climatol.*, **52**, 1803–1816, https://doi.org/10.1175/JAMC-D-12-0125.1.

Yang, T. W., M. T. Lü, S. Q. An, and D. H. Zhao, 2014: Comparison of near-ground ozone concentrations between urban and rural forests. *Acta Ecologica Sinica*, **34**, 5670–5678, https://doi.org/10.5846/stxb201301150104. (in Chinese with English abstract)

Yue, X., and Coauthors, 2017: Ozone and haze pollution weakens net primary productivity in China. *Atmospheric Chemistry and Physics*, **17**, 6073–6089, https://doi.org/10.5194/acp-17-6073-2017.

Zhang, Y. L., and F. Cao, 2015: Fine particulate matter ($PM_{2.5}$) in China at a city level. *Sci Rep*, **5**, 14884, https://doi.org/10.1038/srep14884.

Zhao, X. L., W. Q. Zhou, and L. J. Han, 2019: Human activities and urban air pollution in Chinese mega city: An insight of ozone weekend effect in Beijing. *Physics and Chemistry of the Earth, Parts A/B/C*, **110**, 109–116, https://doi.org/10.1016/j.pce.2018.11.005.

Zhao, Y., J. Zhang, and C. P. Nielsen, 2013: The effects of recent control policies on trends in emissions of anthropogenic atmospheric pollutants and CO_2 in China. *Atmospheric Chemistry and Physics*, **13**, 487–508, https://doi.org/10.5194/acp-13-487-2013.

Zheng, J. Y., L. J. Zhong, T. Wang, P. K. K. Louie, and Z. C. Li, 2010: Ground-level ozone in the Pearl River Delta region: Analysis of data from a recently established regional air quality monitoring network. *Atmos. Environ.*, **44**, 814–823, https://doi.org/10.1016/j.atmosenv.2009.11.032.

Zheng, Z. F., and Coauthors, 2018: Relationship between fine-particle pollution and the urban heat island in Beijing, China: Observational evidence. *Bound.-Layer Meteorol.*, **169**, 93–113, https://doi.org/10.1007/s10546-018-0362-6.